ISSN: 1672 - 6553

JOURNAL OF DYNAMICS AND CONTROL

VOLUME 9 ISSUE 10: 37-43

# BAND-GAP, THICKNESS AND DOPING CONSIDERATION FOR CIGS/ZNS/ZNO CELL USING SCAPS-1D

Satyendra Kumar, Swati Arora

Swami Keshvanand Institute of Technology, Management & Gramothan, Jaipur, India

JOURNAL OF DYNAMICS AND CONTROL
https://doi.org/10.71058/jodac.v9i10006

# BAND-GAP, THICKNESS AND DOPING CONSIDERATION FOR CIGS/ZNS/ZNO CELL USING SCAPS-1D

**Satyendra Kumar, Swati Arora**

*Swami Keshvanand Institute of Technology, Management & Gramothan, Jaipur*
*rajeshwar.satyendra@gmail.com, swati@skit.ac.in*

***Abstract*-- Solar energy is rendered useful among renewable energy in India. The government has launched a National Solar Mission to meet future demands for electricity. The favorable condition in throughout the country provides enormous scope for research and development. This work is aimed to fine-tune design parameters like band-gap, doping concentration and thickness of CIGS absorber to enhance the energy conversion per unit cell. For this a laboratory reference model was considered. A precise and correlated simulation model is designed using SCAPS-1D. Effects of optimization of its parameters are studied where band gap of CIGS is varied in the range 1.040eV to 1.411eV, doping consideration from 1015 (/cm3) to 1017 (/cm3) and thickness of CIGS layer from 0.5µm to 2µm. Number of iterations of simulations are performed to precise the open circuited voltage and short-circuited current density. Another objective of this work was to replace toxic Cd by a suitable compound. A well extracted ZnS of are incorporated with different compositions to propose an optimized CIGD/ZnS/ZnO structured solar cell. The 26.82% efficiency (best performance) achieved at band-gap 1.268eV, acceptor concentration $10^{15}$(1/cm$^3$), and thickness 1.5µm with buffer $Zn_{1-y}S:Cu_y$ at y=0.06 which is 28.55% higher than that of reference cell.**

***Index Terms*—Solar energy, Energy Conversion, Voltage, Current Density, Band Gap, Doping Concentration, CIGS, SCAPS-1D.**

## NOMENCLATURE

A = Diode ideality factor
K = Boltzmann Constant
T = Substrate Temperature in Kelvin
q = Quantum electronic charge.
G = Incident Solar Irradiated Power per unit area
λ = Wavelength of Irradiations
F = Incident Solar Flux per unit area

## I. INTRODUCTION

Solar cell is a device or basically a semiconductor diode which converts solar energy into electric energy. Theory of this phenomenon is well explained by photoelectric effect. According to which energy received or released by electrons or must be integral of quantum energy hυ. The cell is categorized on the basis of materials, and fabrication techniques used. Thin film solar cell generally usage alloy type compound materials like CIGS/CIGSSe/CdTe/GaAs/a-Si as active layer. Some of these materials were reviewed by Ramanujam et al. [1]. These materials have their own pros and cons over one another and the same is with different fabrication techniques. The prime challenges are to enhance entire performance metrics of the cell. Most of commercial cells are failed to match the theoretical limit of single junction solar cell efficiency about 30% approximated by W. Shockley, H.J. Queisser [2] and known as SQ-limit of the cell. Tariq AlZoubi et al. [3] reported a simulation efficiency of 21.35% to 24.21%, through optimization of band gap, doping density and thickness of absorption (CIGS) and window (CdS) layers.

Major factors affecting the performance are reduced absorption spectrum as compared to the incident solar spectrum, thermal stabilization loss, absorption into window layer, transmission and reflections from different boundaries of the cell. Various technics and advanced quantum approaches are made by researchers to reach the limiting efficiency. The maximum efficiency reached with single junction thin film solar cell in authentic laboratory is about 20%-to-23.4% reviewed by Maalouf et al. [4] and Ali et al. [5]. Deposition of an extra layer/sensitizer/concentrator increases cost of production corresponding to insignificant increment in efficiency. On other hand thin film solar cell materials like Cadmium and Telluride are found toxic and hazardous as introduced by Vasilis M. Fthenakis [6] so efforts are being made to minimize their use or replace with other materials. This work aims to improve the performance without increasing the cost of production and minimizing toxicity by replacing such materials with suitable compounds. The similar approach was made with kesterrite CZTS as active layer and ZnS as window layer explored by Satyendra Kumar and Swati Arora [7] where efficiency reportedly improved with respect to conventional CZTS solar cell. But, it is less than that of CIGS cell. It has also been reported in conference proceedings (ICANCT-2021) by Satyendra Kumar and Swati Arora[8] that optimization of thickness of buffer layer also can enhanced the efficiency of the cell. The performance of unit cell is determined through four parameters metrics 1. $V_{oc}$, 2. $J_{sc}$, 3. Fill Factor and 4. Efficiency η; irrespective of the type of solar cells used mentioned by

Satyendra Kumar is research scholar at research center Department of Electronics Engineering, Swami Keshwanand Institute of Technology, Management & Gramothan, Jaipur, India-302017, and enrolled at Department of Electronics and Communication Engineering, Rajasthan Technical University, Kota, Rajasthan, India (e-mail: rajeshwar.satyendra@gmail.com).

Swati Arora, is with Department of Electronics Engineering, Swami Keshwanand Institute of Technology, Management & Gramothan, Jaipur, India-302017 (e-mail: swati@skit.ac.in).

https://doi.org/10.71058/jodac.v9i10006

Angel Antonio and Bayod-Rújula [9].

Efficiency (η) of a cell is determined through the ratio of electrical power produced to that of incident solar irradiance on the cell per unit area expressed as

$$\eta = \frac{P_{max}}{G} \times 100\% = \frac{V_{oc} \times J_{sc} \times FF}{P_{in}} \times 100\% \quad (1)$$

Here, $V_{oc}$ represents Open-Circuited Voltage, $J_{sc}$ Short-Circuited Current Density and FF to Fill Factor of the cell. These metrics depend on various parameters of device and further defined as

$$V_{oc} = \frac{AKT}{q} \ln\left(\frac{I_L}{I_o} + 1\right) \quad (2)$$

(2)

Where, A denotes diode ideality factor, $I_L$ photo-current and $I_o$ reverse saturation current. Here, $V_{oc}$ is not dependent on temperature only but it also depends on $I_L$. Because, $V_{oc}$ tends to zero in absence of light therefore, its maximum value can be approximated as $V_{oc}$=0.693 ×AKT/q.

$V_{oc}$ defines the output voltage produced by a cell when there is no load connected to it. $J_{sc}$ represents maximum current per unit area generated by unit solar cell when load of the device is short-circuited. FF defines the maximum possible power measured to the (ideal) maximum power = $V_{oc} \times J_{sc}$ that can be generated by a cell whereas efficiency defines maximum power drawn by a load from the unit cell.

Fig. 1 represents a layered structure of CIGS thin film single junction solar cell. Here, thickness of active layer reportedly found in the range of 0.5µm to 4µm, that of buffer layer 30-60nm and trans-conductance-oxide layer about 0.200µm. Molybdenum and Aluminum are used for front and back contacts respectively.

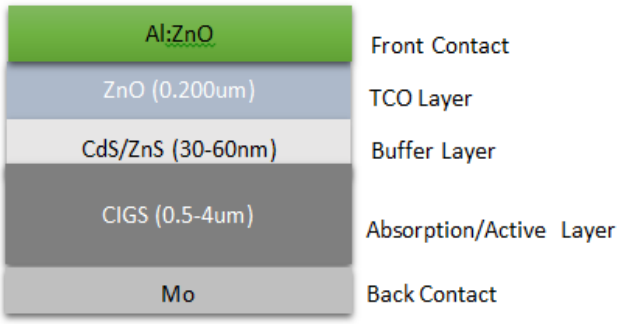


**Fig. 1 Structure of single-junction thin film solar cell**

## II. THEORY

The Photo-Current-Density $J_L$ of diode (single junction solar cell) can be assumed to be sum of hole-current-density $J_p(\lambda)$ in buffer region, $J_r(\lambda)$ recombination-current-density in space charge region and $J_n(\lambda)$ electron-current-density in active region. These components defined through equations (3) to (5) mentioned by Condia et al. [10], Abdelkader benmir and Mohammad Salah Aida [11].

$$J_p(\lambda) = \frac{(q \times F(\lambda) \times (1-R) \times \alpha_1 \times w_p)}{(\alpha_1 \times w_p)^2 - 1} \times \left[\frac{\frac{v_p \times w_p}{k_p} + e^{-\alpha_1 w_n}\left(\frac{v_p \times w_p}{k_p}\cosh\left(\frac{x_n}{w_p}\right) + \sinh\left(\frac{x_n}{w_p}\right)\right)}{\frac{v_p \times w_p}{k_p} \times \sinh\left(\frac{x_n}{w_p}\right) + \cosh\left(\frac{x_n}{w_p}\right)} - \left(\alpha_1 \times w_p \times e^{-\alpha_1 x_n}\right)\right] \quad (3)$$

$$J_n(\lambda) = \frac{(q \times F(\lambda) \times (1-R) \times \alpha_2 \times w_n)}{(\alpha_2 \times w_n)^2 - 1} \times \left[\alpha_2 \times w_n - \frac{\frac{v_n \times w_n}{k_n}\left(\cosh\left(\frac{x_p}{w_n}\right) - e^{-\alpha_2 x_p}\right) + \sinh\left(\frac{x_p}{w_n}\right) + \alpha_2 \times w_n \times e^{-\alpha_2 x_p}}{\frac{v_n \times w_n}{k_n} \times \sinh\left(\frac{x_p}{w_n}\right) + \cosh\left(\frac{x_p}{w_n}\right)}\right] \times e^{-(\alpha_1 l_1 + \alpha_2 l_2)} \quad (4)$$

$$J_r(\lambda) = q \times F(\lambda) \times (1-R) \times e^{-\alpha_1 x_n} \times (1 - e^{-\alpha_1 r_1 - \alpha_2 r_2}) \quad (5)$$

Here, 'F' denotes to solar flux nearby cell substrate, R to reflectivity, '$w_n$' and '$w_p$' to diffusion length for n-type and p-type charge carriers; '$x_n$' and '$x_p$' to length of n-type and p-type neutral regions; '$k_n$' and '$k_p$' to diffusion coefficients; '$v_n$' and '$v_p$' to recombination speed of electrons and holes; '$\alpha_1$' and '$\alpha_2$' to absorption coefficients; '$r_1$' and '$r_2$' space charge regions, and '$l_1$' and '$l_2$' to total length of n-type ZnS and p-type CIGS respectively.

When irradiations incident on front surface of solar cell, transmissions, reflections and absorptions of light energy take place at interfaces of the materials starting from air-ITO, to ITO-ZnS, ZnS-CIGS, CIGS-Mo and Mo-Air as well as at front and back contacts as discussed by Zhiming xu et al. [12] and Sylvère Leu et al.[13]. These phenomena turned down efficiency of the cell at greater extent. Because, percentage of irradiations of solar energy reached to the active region after passing through multiple layers is not being absorbed completely in any material. Also what absorbed is not hundred percent contributed into current. Thus to step up the deliverable output power of the solar cell without increasing fabrication steps and cost of the fabrication, optimization to achieve precise material configurations are preferred.

The band gap of a material determines absorption of solar flux or energy into the material. Consequently it generates charge carriers into the regions which may vary slightly with temperature of the material. Here the temperature near substrate of the material assumed to be fixed at 300 K.

$$\alpha_2 \propto \sqrt{E - E_{CIGS}} \quad (6)$$

The maximum open circuit voltage of the cell depends on photo current generated, as temperature of substrate is kept constant whereas reverse saturation current also fixed for a specific cell. Hence, it depends on decisive design parameters like diffusion length, effective doping concentrations and band gap of anode and cathode regions. Lifetime of charge carrier ensures, their velocities and thickness of the layers affects the current densities in subsequent regions as defined in equations

https://doi.org/10.71058/jodac.v9i10006

(3) to (5) and recombination in neutral regions. Therefore, it short circuit current of the cell is also affected. Diffusion length '$w_n$' and '$w_p$' of electron and holes respectively depend on concentrations of acceptor and donor impurities and also on effective concentrations in conduction and valance bands of the materials. Diffusion length of charge carrier is defined by (7).

$$w = w(N_A, N_D, \epsilon_1, \epsilon_{2,} V_d) \quad (7)$$

Where $V_d$ denotes contact potential of the diode and $\epsilon_1, and\ \epsilon_2$ to electric permittivity of the material. Therefore, acceptor and donor concentration affects diffusion length which consequently affect the fill factor (flatness of V/I characteristics) of the cell.

## III. Methodology

It has been explored into introduction section of this report that how $V_{oc,}$ $J_{sc,}$ and FF depends on bandwidth, thickness and density of donor/acceptor atoms. Therefore, it is wisely proposed to determine the optimal values for these parameters and their incorporation into modeling of the cell will definitely improve overall performance of the cell. The model to be evaluated should follow the characteristics of laboratory or industrial thin film solar cell very closely. Therefore, reference models of the solar cells reported by Ali et al. [3], Sayeed et al. [14], Osman et al. [15] and also by Asaduzzaman et al. [16] have been simulated successfully through SCAPS-1D. The performance gap is minimized between laboratory solar cell and SCAPS model of the reference cell by selecting appropriate absorption model, value of physical parameters, series and shunt resistances, temperature, transmittance and others. The response of laboratory reference CIGS thin film solar cell and that of its simulation model have area 0.410cm$^2$ and thickness d=1μm are presented in table 1.

**Table 1 Simulation of reference model CIGS thin film solar cell**

| Material | $E_g$(eV) | $N_a$ ($cm^{-3}$) | $V_{oc}$ (V) | $J_{sc}$ ($ma.cm^{-2}$) | η % |
|---|---|---|---|---|---|
| Ref.[3] | 1.04-1.67 | $10^{14}$-$10^{18}$ | 0.6-0.8 | 32-40 | 21-24 |
| Sim. | 1.186 | $5*10^{16}$ | 0.70 | 35.6 | 20.77 |

The above model is simulated at room temperature 300 K, series resistance 0.5Ω, shunt resistance 1000Ʊ, and irradiance spectrum model AM1.5[17] using SCAPS-1D simulator. Band gap $E_g = 1.040eV$, Electron affinity $\chi_a = 4.5eV$, relative permittivity $\epsilon_r = 14$, thermal velocity of electrons and holes $10^7 cm/s$, electrons mobility 100 ($cm^2$/Vs) and holes mobility 25($cm^2$/Vs) for CIGS layer..

According to theory of photoelectric effect the absorption of solar energy (photons) into materials widely depends on fundamental frequency of oscillations of atoms/molecules of the materials. Therefore, a material whether having crystalline or non-crystalline structure absorbs only those photons which contain energy larger than threshold energy ($h\upsilon_o$) of the oscillatory atoms or molecules. Consequently, irradiations spectrum of wavelength in certain range depending on material property is absorbed which in turn determine absorption co-efficient α (1/m) while rest part of irradiation energy lost. The precise band gap of polycrystalline semiconductor materials can be obtained through controlled doping concentration into the material. Hence, for better optimization of band gap precise extraction of absorption model is essential. So that it's performance metrics should follow that of real or experimental characteristics of the cell. Thus, an accurately extracted and laboratory established model of absorption constants corresponding to various doping concentration of CIGS thin layer reported by P.D. Paulson et al.[17], and Hulstrom et al. [18] are taken into consideration to propose this model. The $\alpha -$spectrum corresponding to various composition of Cu-doping concentration x=0.31, x=0.45, and x = 0.66 are plotted in Fig. 2. It is widely established fact that there is major loss of energy $h(\upsilon - \upsilon_0)$ corresponding to short waves in terms of thermal loss.

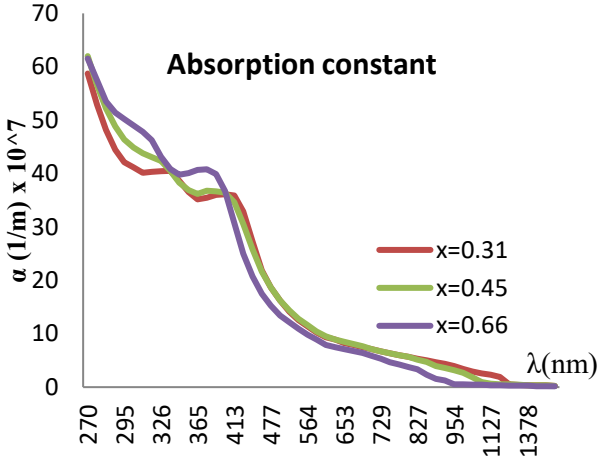


**Fig. 2 Absorption characteristics of CIGS thin film**

To overcome these losses photon down conversion/downshifts are suggested in reports of Mora et al. [19] but, it has not included in scope of this work. Band gap of p-type CIGS for x=0.0 to 0.50 is approximated by (8) and tuned precisely in the range 1.040eV to 1.30eV [20]. The loss can further be minimized by selecting appropriate absorption model. Therefore, absorption model having wider spectrum bandwidth and higher absorbance values of α (1/m) for longer wavelength is preferred.

$$E_g = 1.040 + 0.391x + 0.262x^2 \quad (8)$$

$$\chi_g = 4.61 - (1.162 \times x) + (0.034x^2) \quad (9)$$

The Simulation is performed corresponding to different configurable band gap of Cu ($In_{1-x}$ $Ga_x$ ) $Se_2$. For the given physical parameters of the cell, précised band gap $E_{g=}$ 1.268eV, electron affinity $\chi_a = 4.093eV$ and efficiency $\eta =$ 23.45% are observed as displayed in table 2 at x=0.45 for Cu ($In_{1-x}$ $Ga_x$) $Se_2$. This result is correlated to world record efficiency of fabricated alloy based thin film solar cell by Nakamura et al. [20] and Abdalmageed et al. [21] with insertion of reflecting layer.

https://doi.org/10.71058/jodac.v9i10006

Table 2 Simulation of CIGS/CdS/ZnO solar cell verses band gap

| X | $E_g$(eV) | $\chi_g$(eV) | $V_{oc}$ (V) | $J_{sc}$ (mA.cm$^{-2}$) | FF (%) | η (%) |
|---|---|---|---|---|---|---|
| 0.0 | 1.040 | 4.610 | 0.55 | 36.16 | 54.68 | 12.06 |
| 0.31 | 1.186 | 4.253 | 0.70 | 35.65 | 75.39 | 20.77 |
| 0.45 | 1.268 | 4.093 | 0.78 | 35.81 | 75.43 | 23.45 |
| 0.50 | 1.30 | 4.03 | 0.85 | 28.50 | 76.94 | 20.76 |

Now, Doping concentration of CIGS is varied and models are simulated at x=0.45, $E_g$=1.268eV to tune it for improved power conversion efficiency. A number of models of doping concentration ranges between 1 x $10^{15}$ / cm$^3$ to 1 x $10^{17}$ / cm$^3$ are considered. It observes decline into efficiency of the cell due to prima facie decline in short circuited current. This decrement in current density is caused by increased recombination in the neutral region of the material. Studies on corresponding four relevant models are represented in table 3.

Table 3 Effect of variation in acceptor doping concentration of CIGS solar cell

| $E_g$ (eV) | $N_a$(cm$^{-3}$) | $V_{oc}$ (V) | $J_{sc}$ (mA.cm$^{-2}$) | FF (%) | η (%) |
|---|---|---|---|---|---|
| 1.268 | 1*$10^{15}$ | 0.79 | 40.88 | 70.16 | 25.22 |
| 1.268 | 1*$10^{16}$ | 0.75 | 38.89 | 73.94 | 23.97 |
| 1.268 | 5*$10^{16}$ | 0.78 | 35.81 | 75.43 | 23.45 |
| 1.268 | 1*$10^{17}$ | 0.79 | 34.26 | 76.64 | 23.25 |

After confinement of $E_g$ and $N_a$, thickness of CIGS layer is investigated to receive optimum power conversion efficiency with similar constraints, like series resistance, shunt resistances and cost of fabrication. For this, Band gap $E_g = 1.268eV$ and doping concentration $N_a = 1 \times 10^{15}(1/cm^3)$ are kept constant while thickness ($d_{CIGS}$) is varied ranging from 0.5µm to 2µm.

Another objective of this work was to make the device Cd-free. Therefore, CdS is replaced by ZnS buffer. For this, characterization of ZnS extracted by Mehdi Hasan et al. [22] is considered to incorporate for SCAPS-1D simulation of optimized CIGS cell. Where, thickness of ZnS layer, and doping of donor concentration $N_d$ are chosen same as that of CdS. Other parametric sets of values needed for modeling in SCAPS-1D are considered on its merit for the device. There are six sets of values of optical and electrical parameters were extracted for Zn1-yS:Cuy against y=0%, 2%, 4%, 6%, 8% and 10%. CIGS layer was considered as p-type so ZnS has to be n-type. Thus, modeling with pure compound y=0% is eliminated although providing highest transmittance value. Similarly, compound with donor doping concentration y = 10% is discarded due to lower transmittance value Γ<66% and increased absorbance in the buffer region. Other four sets of values of modeling parameters corresponding to y=2%, 4%, 6% and 8% are considered to get the précised and improved response.

## IV. Results & Discussion

Tuning of $E_g, N_a$ and d parameters of CIGS absorber layer have improved the values of performance metrics as characterized into Fig. 3 to Fig. 6. Fig. 3 represents variation in $V_{oc}$ corresponding to $E_g, N_a$ and d. It shows that $V_{oc}$ increases with $E_g$ but after certain value of $E_g = 1.186eV$ rate of increment in $V_{oc}$ slows down by almost 16%. When $V_{oc}$ verses $N_a$ curve is explored then it is found that after initial slows down from $N_a = 10^{15}$ (1/cm$^3$) to $10^{16}$ (1/cm$^3$) it becomes consistent and there is very small change in $V_{oc}$ corresponding to variation in $d$ is observed.

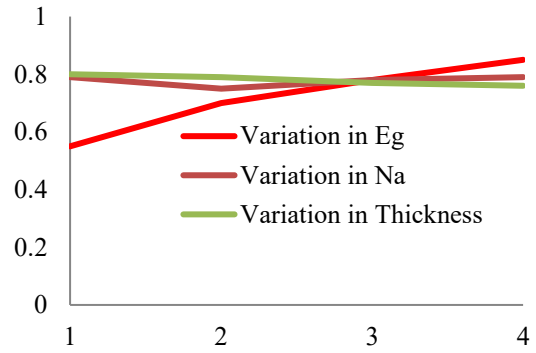


Fig. 3 Open circuit voltage characteristics verses band gap, donor concentration and thickness of CIGS

Current density curves verses $E_g/N_a/d$ are characterized in Fig. 4. $J_{sc}$ verses $E_g$ characteristic curve shows that $J_{oc}$ remains constant for $E_g$ <=1.268eV and decreases beyond that. While it is started decreasing in $J_{sc}$ verses $N_a$ just after $N_a$ =$10^{16}$ (1/cm3). Whereas it increased when thickness increases from 0.5<= d<=1.5µm and starts decreasing after d>=1.5µm.

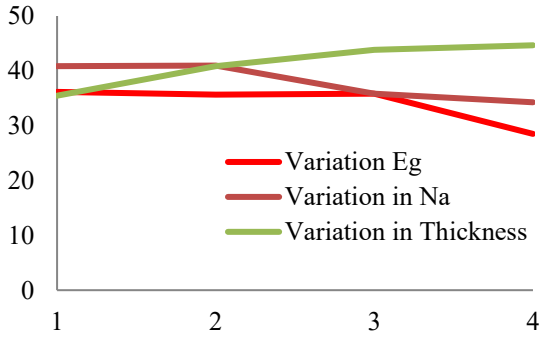


Fig. 4 Short-circuited current density characteristics verses band gap, donor concentration and thickness of CIGS

Fill factor curves depicts in Fig. 5 where it is found that FF approximately same against variation in $E_g$ and $N_a$ in the range 1.186eV<= Eg <=1.30eV, and $10^{16}$(1/cm$^3$) <= $N_a$ <= $10^{17}$(1/cm$^3$) respectively. While it starts decreasing when thickness increases from 0.5µm to 2µm. corresponding to

https://doi.org/10.71058/jodac.v9i10006

variation in thickness 0.5µm<=d>=2µm. This small decrement in fill factor less impacted the overall performance of the cell.

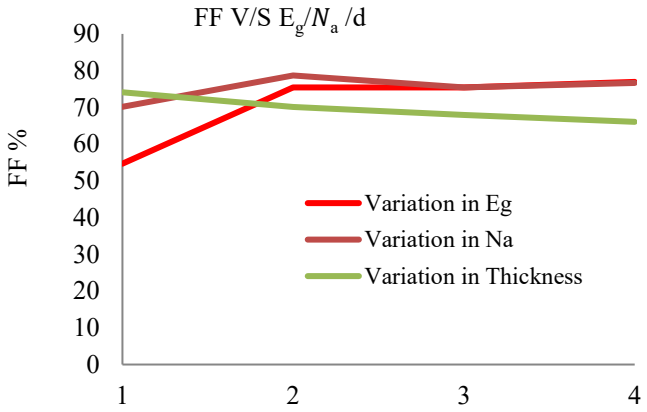


Fig. 5 Fill Factor characteristics verses band gap, donor concentration and thickness of CIGS

Fig. 6 reflects efficiency of the cell. It increase with $E_g$ in the range of 1.040eV<=$E_g$>=1.268eV and decreases when $E_g$ increased further. While it decreases with increase in doping concentration in the range $10^{15}(1/cm^3)$ <=$N_a$<=$10^{16}(1/cm^3)$ and becomes constant thereafter. Whereas η increases when thickness increased in the range 0.5µm<=d<=1.5µm and decreases beyond d>1.5µm.

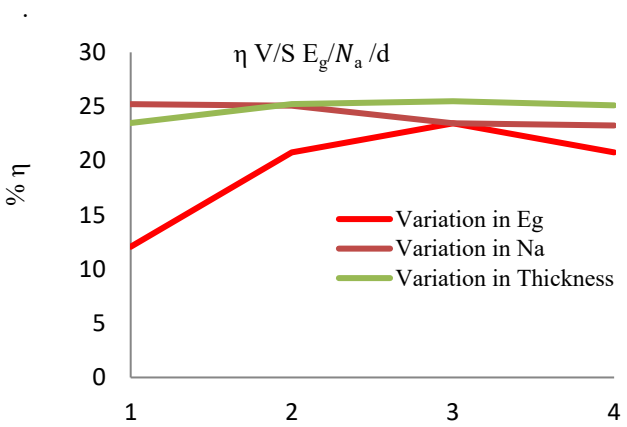


Fig. 6 Efficiency characteristics verses band gap, donor concentration and thickness of CIGS

When all the performance parameters are analyzed together, then it is observed that tuning bandwidth to 1.268eV optimized $V_{oc}$, as it also provides highest efficiency and current density for the model. Then keeping it fixed and tuning $N_a$ to $10^{15}$ (/cm) improved $J_{sc}$ further while $V_{oc}$ remains comparable. The current density enhanced again by some extent when tuning its thickness to 1.5µm. optimization of $V_{oc}$ and $J_{sc}$ optimizes the efficiency to its optimum value as described in table 4.

Table 4 Thickness Optimization results of CIGS layer

| $E_g = 1.268eV$, $N_a = 1 \times 10^{15}(1/cm^3)$ | | | | |
|---|---|---|---|---|
| $d_{CIGS}$ (µm) | $V_{oc}$ (V) | $J_{sc}$ (mA.cm$^{-2}$) | FF (%) | η (%) |
| 0.5 | 0.8 | 35.47 | 74.11 | 23.48 |
| 1 | 0.79 | 40.88 | 70.16 | 25.22 |
| 1.5 | 0.77 | 43.8 | 67.9 | 25.49 |
| 2 | 0.76 | 44.66 | 66.07 | 25.11 |

Fig. 7 shows that power generation ($V_{oc} \times J_{sc} \times FF$) by unit solar cell. It increases with increase in thickness of CIGS layer from $t_{CIGS} = 0.5\mu m$ to $1.5\mu m$ and starts decreasing afterward. The observations suggest that performance is optimum at $E_g$ =1.268eV , $Na = 1 \times 10^{15}$ (1/cm$^3$) and d = 1.5µm attain $V_{oc} = 0.77V$ , $J_{sc} = 43.80$ (mA/cm$^2$), FF=67.90%, and η = 25.49% with possible deviation of ±1.5% and proved to be the highest performance achieved for a single junction CIGS/CdS/ZnO thin film solar cell without using any concentrator, reflector or photon conversion layer.

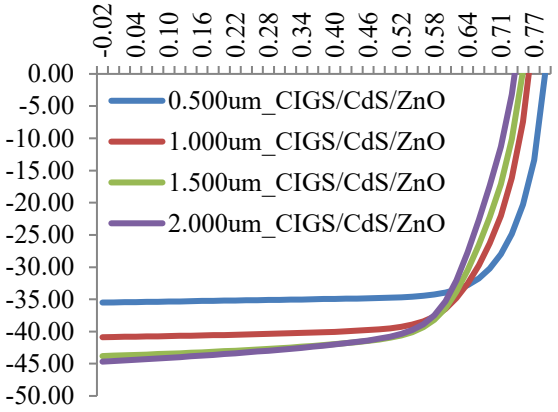


Fig. 7 Comparison of performance of CIGS solar cell using CdS and ZnS as buffer layer

The optimized configuration of CIGS layer is used ahead for modeling of CIGS/$Zn_{1-y}S$: $Cu_y$/ZnO cell. The simulation results of Cd-free solar cell are sum up in table 5.

Table 5 Performance of CIGS/ZnS/ZnO structured solar cell

| y(%) | $V_{oc}(V)$ | $J_{sc}(\frac{mA}{cm^2})$ | FF (%) | η (%) |
|---|---|---|---|---|
| 2 | 0.78 | 45.12 | 67.23 | 26.32 |
| 4 | 0.78 | 45.18 | 67.76 | 26.67 |
| 6 | 0.79 | 45.22 | 67.99 | 26.82 |
| 8 | 0.78 | 45.17 | 67.84 | 26.71 |

This result found considerable as ZnS is more transparent to solar irradiations as compared to CdS therefore, energy penetration and advancement at absorber layer is expected. This is due to higher band gap (>3.44eV) between valance band and conduction band of ZnS as compared to that of CdS (2.5eV). Less doped n-type ZnS offers less charge density therefore recombination in space charge region reduced consequently low charge density of the cell is observed. When donor doping

https://doi.org/10.71058/jodac.v9i10006

concentration is increased, the local charge career initially increases while absorbance in the region also increased and transmittance of the material decreases. When this doping concentration increased after certain level the absorbance and transmittance collectively in the region becomes significant and so again current density in n-region starts to decrease due to increased recombination in neutral region of the buffer. Therefore, results at y=6%, is found best suitable solution for optimized CIGS/$Zn_{1-y}S$: $Cu_y$/ZnO thin film solar cell.

Fig. 8 provides comparative study of VI-characteristics among CIGS/CdS/ZnO reference cell (A), optimized CIGS/ZdS/ZnO reference cell (B) and Cd-free proposed CIGS/ZnS/ZnO cell (C). It also indicates improvements in Voc , Jsc , Fill Factor (flatness of VI-curve near Voc) and so efficiency of the optimized CIGS cell with ZnS as buffer layer.

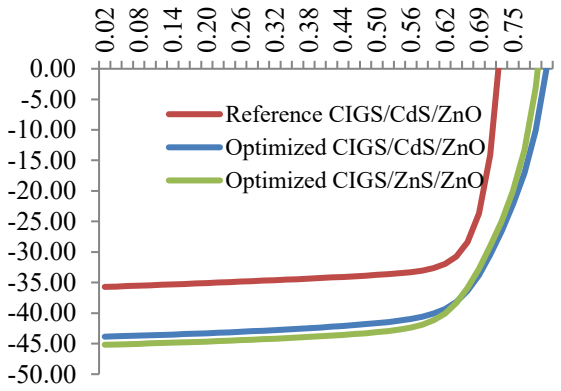


**Fig. 8 Comparison of performance of CIGS solar cell using CdS and ZnS as buffer layer**

## V. Conclusion

Major objective of presented work was confinement of physical parameters and replacement of toxic Cd from the cell in order to provide environment friendly and more efficient model of CIGS based polycrystalline solar cell. To make it Cd-free cell, there are number of possible choices available like ZnS, ZnSn, InP, and others. The stability, robustness, availability and tunable band gap of ZnS make it suitable for the application. Higher transmittance for irradiated solar spectrum, wider band gap and lower absorbance of ZnS boosted most of the performance-metrics of the cell. The result summarized in table 6. It provides relative increment of 12.14% in $V_{oc}$ , 26.84% in $J_{sc}$ and 29.12% in η whereas 9.80% decrement in FF. There is still a scope of improving these performance parameters by adopting concentrators, reflectors and photon conversion layers.

**Table 6 Performance of optimized toxic free CIGS/ZnS/ZnO thin film solar cell**

| Cell | $E_g$ (eV) | $N_a$ ($cm^{-3}$) | d ($\mu m$) | $V_{oc}$ (V) | $J_{sc}$ ($mA.cm^{-2}$) | FF (%) | η (%) |
|---|---|---|---|---|---|---|---|
| **A** | 1.11 | $5*10^{16}$ | 1 | 0.70 | 34.60 | 75.4 | 20.77 |
| **B** | 1.26 | $1*10^{15}$ | 1.50 | 0.77 | 43.8 | 67.9 | 25.49 |
| **C** | 1.26 | $1*10^{15}$ | 1.50 | 0.79 | 45.22 | 68.0 | 26.82 |

## VI. Acknowledgment

We are thankful to Marc Burgelman, honarary professor University of Gent, ELIS, Campus Ardoyen, Technologiepark 914, Grote Steenweg for providing the simulator which helps immensely to find the optimum solution.

## VII. References

[1] Jeyakumar Ramanujam, Douglas M. Bishop,Teodor K. Todorov, Oki Gunawan, Jatin Rath, Reza Nekovei, Elisa Artegiani, Alessandro Romeo, (2020), Flexible CIGS, CdTe and a-Si:H based thin film solar cells: A review, *Proogress in Material Science, Elsevier, Vol 110;*Available: https://doi.org/10.1016/j.pmatsci.2019.100619

[2] W. Shockley, H.J. Queisser,( 1961), Detailed balance limit of efficiency of p-n junction solar cells, *J. Appl. Phys., Vol. 32;* Available: https://doi.org/10.1063/1.1736034

[3] Tariq AlZoubi, M. Moustafa, (2019), Numerical optimization of absorber and CdS buffer layers in CIGS solar cells using SCAPS, *International Journal of Smart Grid and Clean Energy 8(3);* Available: https://doi.org/ 10.12720/sgce.8.3.291-298

[4] Amani Maalouf, Tobechi Okoroafor, Zacharie Jehl, Vivek Babu, Shahaboddin Resalati, (2023), A comprehensive review on life cycle assessment of commercial and emerging thin-film solar cell systems, *Journal of Renewable and Sustainable Energy Reviews, Elsevier, Vol 186*; Available: https://doi.org/10.1016/j.rser.2023.113652

[5] N. Ali, A. Hussain, R. Ahmed, M.K. Wang, C. Zhao, B. Ul Haq, Y.Q. Fu, (2016 ), Advances in nanostructured thin film materials for solar cell applications, *Journal of Renewable and Sustainable Energy Reviews, Elsevier, Vol 59;* Available: https://doi.org/10.1016/j.rser.2015.12.268

[6] Vasilis M. Fthenakis, (2012) , *Practical Handbook of Photovoltaics* (Second Edition); Wiley, Available: https://doi.org/10.1016/C2011-0-05723-X

[7] Satyendra Kumar, Swati Arora, (2022), Performance Enhancement of Kesteite Cu2ZnSn(S,Se)4 Thin Film Solar Cell, *International Conference on Automation, Computing and Renewable Systems ICACRS, IEEE,* Available: https://doi.org/10.1109/ICACRS55517.2022.10029015

[8] Satyendra Kumar, Swati Arora, (2021 ), Effect of Buffer Layer on Cu(In, Ga)Se2 Solar Cell Performance, *presented at Conference ICANCT-2021;* Available: https://doi.org/10.47904/IJSKIT.11.3.2021.20-24

[9] Angel Antonio Bayod-Rújula, (2019), Solar Hydrogen Production, *Processes Systems and Technology,* Available: https://doi.org/10.1016/B978-0-12-814853-2.00008-4

[10] Bernal-Condia, J A S´anchez-Cely, J D Bastidas-Rodriguez, M A Botero-London˜o and M A Mantilla-Villalobos; (2019), Simulation of a thin-film solar cell based in kesterite using Matlab, *Journal of Physics: Conf. Series 1159;* Available: https://doi.org/10.1088/1742-6596/1159/1/012020

https://doi.org/10.71058/jodac.v9i10006

[11] Abdelkader benmir, Mohammad Salah Aida, (2016), Simulation of a thin-film solar cell based on Copper Zink Sulpho-Selenide Cu2ZnSn(S,Se)4, *Superlattices and microstructures, Elsiever;* Available: https://doi.org/10.1016/j.spmi.2015.12.027

[12] Zhiming xu, Hongwei qu, Xingcan li, Yu zhao, Yuchen li, Zhimin han, Theoretical model of optical transmission and reflection characteristics of dusty PV modules, *Journal of Solar Energy Materials and Solar Cells, Elsevier, Vol. 213*; 2020 doi.org/10.1016/j.solmat.2020.110554

[13] Sylvère Leu, Detlef Sontag, (2020), Solar Cells and Modules: Optical and Recombination Losses, *SSMATERIALS,Spriger, Vol 301,* Available: https://doi.org/10.1007/978-3-030-46487-5

[14] Abu Sayeed, Md., Rouf, H.K., (2019 ), Numerical simulation of thin film solar cell using SCAPS-1D:ZnSe as window layer, presented at *(ICCIT-2019), IEEE;* Available: https://doi.org/10.1109/ICCIT48885.2019.9038584

[15] Yasmina Osman, Mostafa Fedawy, Mohamed Abaza, Moustafa H. Aly, (2021), Optimized CIGS based solar cell towardsan efficient solar cell: impact of layers thickness and doping, *Journal of Optical and quantum Electronics, Springer, Vol. 53;* Available: https://doi.org/10.1007/s11082-021-02873-4

[16] Md. Asaduzzaman, Mehedi Hasan, Ali Newaz Bahar, (2016), An investigation into the effects of band gap and doping concentration on Cu(In,Ga)Se2 solar cell efficiency, *Springerplus;* https://doi.org/10.1186/s40064-016-2256-8

[17] P.D. Paulson, R.W. Birkmire, W.N. Shafarman, (2003), Optical characterization of CuIn1-xGaxSe2 alloy thin films by spectroscopic ellipsometry, *Journal of Applied Physics, Vol 94;* Available: https://doi.org/10.1063/1.1581345

[18] Hulstrom, Bird and Riordan, (1995), *Solar Cells and their applications,* Wiley, Available: https://doi.org/10.1016/0379-6787(85)90052-3

[19] M.B. de la Mora, O. Amelines-Sarriac, B.M. Monroy, C.D. Hernández-Pérez, J.E. Lugo, 2017 Materials for downconversion in solar cells: Perspectives and challenges, *Journal of Solar Energy Materials and Solar Cells, Elsevier; Vol. 165*, Avaible: https://doi.org/10.1016/j.solmat.2017.02.016

[20] Motoshi Nakamura, Koji Yamaguchi, Yoshinori Kimoto, Yusuke Yasaki, Takuya kato, and Hiroki sugimoto:, (2019 ), Cd-Free CIGSSE Thin-Film Solar Cell World Record Efficiency 23.35%, *IEEE Journal of Photovoltaics, 2156-3381;* Available: https://doi.org/10.1109/JPHOTOV.2019.2937218

[21] Hussan Ismail Abdalmageed, Mostafa Fedawy and Moustafa H. Aly, (2021), Effect of Absorber Layer Band Gap of CIGS-based Solar Cell with (CdS/ZnS) Buffer Layer, *Journal of Physics, IOP;* Available: https://doi.org/10.1088/1742-6596/2128/1/012009

[22] Mahdi Hasan Suhail and Raoof Ali Ahmed, (2014) Structural, Optical and electrical properties of doped copper ZnS thin films prepared by chemical spray pyrolysis technique, *Advances in Applied Science Research, Vol 5;* Available: https://doi.org/10.1016/j.ijleo.2017.10.034